Experimental determination of Γ-*X* intervalley transfer mechanisms in GaAs/AlAs heterostructures

R. Teissier
Laboratoire de Microstructures et Microélectronique, CNRS, 196 Avenue Henri Ravera, 92225 Bagneux, France

J. J. Finley, M. S. Skolnick, and J. W. Cockburn
Department of Physics, University of Sheffield, Sheffield S3 7RH, United Kingdom

J.-L. Pelouard
Laboratoire de Microstructures et Microélectronique, CNRS, 196 Avenue Henri Ravera, 92225 Bagneux, France

R. Grey, G. Hill, and M. A. Pate
Department of Electronic and Electrical Engineering, University of Sheffield, Sheffield S1 3JD, United Kingdom

R. Planel
Laboratoire de Microstructures et Microélectronique, CNRS, 196 Avenue Henri Ravera, 92225 Bagneux, France
(Received 19 March 1996)

Zone-center–zone-boundary (Γ-*X*) intervalley transfer mechanisms in AlAs/GaAs heterostructures are deduced in an unambiguous way from transport and electroluminescence studies of single-AlAs-barrier diodes. We demonstrate that the tunneling is strongly sequential and depends on the nature of the *X* state involved. For X_z the transfer is mainly elastic, whereas momentum conserving phonon assistance is dominant for X_{xy}. Quantitative values for the scattering rates for each transfer mechanism are obtained. The conduction-band offset from the Γ minimum in GaAs to the *X* minimum in AlAs is shown to be only 120 ± 6 meV. [S0163-1829(96)52436-7]

The exact mechanisms governing Γ-*X* intervalley transfer in AlAs/GaAs heterostructures are still subject to controversy. In bulk materials the main intervalley scattering process is zone-edge phonon scattering. By contrast, in a heterostructure the potential modulation along the growth axis induces mixing of the Γ and *X* electronic states and direct transitions can take place. The importance of such mixing has been demonstrated from studies of optical transition lifetimes in type-II superlattices[1,2] (SL's) and from observations of Γ-*X* anticrossing.[3] Real-space electron transfer in such SL's, where electrons are created in the GaAs layers and transfer to *X* in the AlAs, has been studied by time-resolved photoluminescence (PL). Feldman *et al.*[4] proposed that it is either due to LO-phonon scattering or to state mixing, depending upon the width of the layers. However, Deveaud *et al.*[5] found transfer rates incompatible with state mixing but in good agreement with phonon-assisted transfer. Γ-*X* transfer also plays a significant role in perpendicular transport through single or double AlAs tunnel barriers,[6,7] tunneling through excited *X* states being demonstrated.[8,9] The results were explained by a state mixing theory,[10] but only imperfectly.

These strong uncertainties are due to the intrinsically poor spectroscopic resolution of the experimental techniques, which access the integrated transfer and cannot resolve individual mechanisms. In this paper we propose an original continuous wave technique achieving very high spectroscopic resolution while still providing results of high time resolution. It permits the nature of the different transfer channels [elastic or inelastic, involving longitudinal (X_z) or transverse (X_{xy})][1–3,11,12] to be precisely evaluated in indirect-gap single-barrier GaAs/AlAs/GaAs tunneling structures. In addition, it enables us to determine generalized Γ-*X* transfer rates which are in good agreement with earlier time-resolved studies.[4,5]

We study a series of single-barrier diodes, designed to have simple two-dimensional (2D) emitter states [Fig. 1(a)]. The structures are then very similar to type-II SL's, with continuously variable Γ-*X* separation. With increasing bias, the opening of a new transport channel, when the emitter Fermi energy is resonant with an excited *X* state, produces a sudden increase of the differential conductance (σ). The number, position, and amplitude of these thresholds in σ versus bias allows the $\Gamma \rightarrow X$ transport mechanisms and their strengths to be identified. Complementary electroluminescence (EL) measurements are employed to determine the distribution of the *X* point electrons in the AlAs layer. Recombination of hot electrons which are ejected out of the barrier[13] is also observed and permits the nature of the $X \rightarrow \Gamma$ transfer to be determined.

The samples studied are *p-i-n* GaAs/AlAs/GaAs heterodiodes, grown by molecular-beam epitaxy, with three different AlAs layer widths of 60, 80, and 100 Å. They were processed into 200-μm-diameter mesas and consist of the following layers: 0.5-μm $n=2\times10^{18}$ cm^{-3} GaAs buffer, 500-Å $n=1\times10^{17}$ cm^{-3} GaAs, 500-Å $n=3\times10^{16}$ cm^{-3} GaAs emitter, 50-Å undoped GaAs spacer, undoped AlAs barrier, 50-Å undoped GaAs spacer, 0.5-μm $p=1.10^{17}$ cm^{-3} GaAs collector, and 0.5-μm $p=1.10^{18}$ cm^{-3} GaAs top contact. The current versus voltage (*I-V*) and σ-*V* curves at 2 K are presented in Figs. 2 and 3

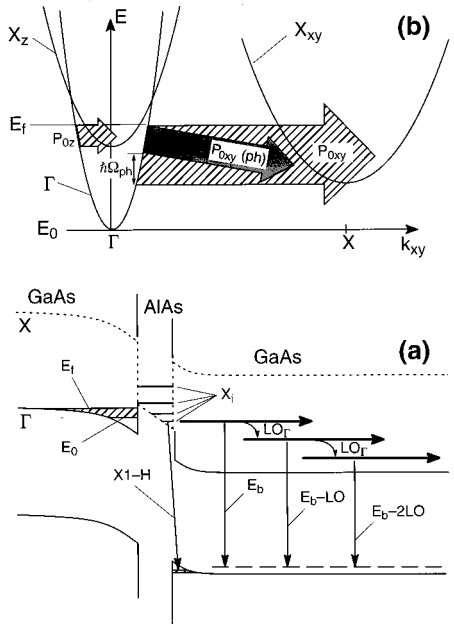

FIG. 1. (a) Schematic band diagram of the structure under forward bias. (b) Schematic dispersion of the 2D emitter and barrier states, showing the elastic and phonon-assisted transfers.

for the three samples. A number of steplike features are observed, each one arising from the opening of a new Γ-X transfer channel. Modeling of the conduction-band profile and of the electronic states is required to identify these features.

The first step in the modeling is a self-consistent solution of Poisson and Schrödinger equations, within the envelope function approximation, as a function of charge density (n_s) in the 2D electron and hole accumulation layers (EAL, HAL). There was assumed to be no charge accumulation in the AlAs layer. We performed current versus magnetic field ($B\|I$) measurements (not presented here) for various biases. The $1/B$ periodicity of the Shubnikov–de Haas–like oscillations in I-B provides a precise determination of n_s for each

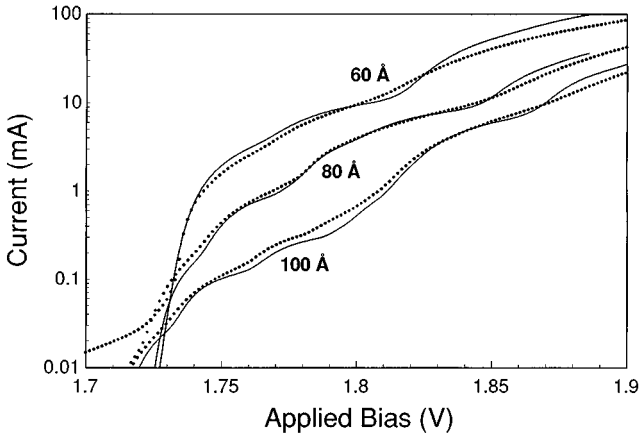

FIG. 2. Measured I-V characteristics for the three samples (dots) and theoretical current (solid lines) from the model parameters described in the text.

V. In addition, the linear variation observed between n_s and V confirms the 2D nature of the emitter states.

The anisotropic conduction-band structure of the AlAs layers was included in the modeling.[1–3,11,12] The opposing effects of quantum confinement and residual uniaxial strain in the AlAs layer[12] lead to the ground electron state being X_{xy}-like for layers thicker than 70 Å, and X_z-like for thinner layers. The X_z and X_{xy} electronic levels and envelope functions were calculated[14] as a function of applied bias. In electric field the overlap of the X wave functions with collector states will be much greater than with emitter states. Thus, transfer out of the barrier is expected to be much more efficient than transfer from the emitter into the barrier. Γ to X transfer into the AlAs is then the current limiting process, and will govern the shape of the I-V characteristic.

We now consider the transfer mechanisms which can occur. Unlike bulk materials, elastic transitions are possible since Γ and X_z states are mixed by the interface potential, and to a lesser extent Γ and X_{xy} are mixed by in-plane potential fluctuations. From PL results on type-II SL's,[2,12] three X point phonons are expected to be involved in the Γ-X transfer: AlAs transverse acoustic ($\hbar\Omega_{\mathrm{TA}}=12$ meV), GaAs longitudinal optic ($\hbar\Omega_{\mathrm{LO,Ga}}=29$ meV), and AlAs longitudinal optic ($\hbar\Omega_{\mathrm{LO,Al}}=48$ meV). Phonon assistance will lead to transfer without conservation of in-plane wave vector (k_{xy}) as will elastic transfer to X_{xy}, since its conduction-band minimum is at large k_{xy}. For Γ-X_z elastic transfer, the heterostructure potential only mixes states with the same k_{xy}. However, interface roughness is likely to induce mixing between states of different k_{xy} [Fig. 1(b)].

Therefore we assume that k_{xy} is not conserved in the transfer, and that Γ-X transfer is governed only by energy conservation [Fig. 1(b)]. The current flowing through level X_i is then given by

$$J_i = eN_s|\langle\Gamma|X_i\rangle|^2 P_0, \tag{1}$$

where N_s is the sheet density of emitter electrons with energy greater than X_i and P_0 is an intrinsic transfer rate which only depends on the nature of the transfer process. The squared overlap of the envelope functions accounts for the spatial separation of the Γ and X 2D states.[4] The total current is the sum of J_i for all X_i levels.[15] Since N_s varies linearly with bias and the overlap is slowly varying, we can approximate σ_i by $\sigma_i \propto |\langle\Gamma|X_i\rangle|^2 P_0$. When a new transfer channel is opened, σ is thus increased by an approximately constant value, proportional to the strength of the transfer process corrected for the overlap. In the following, the exact derivative of (1) was used. Phonon-assisted transitions are included simply by changing the threshold energy X_i to $(X_i + \hbar\Omega_{\mathrm{ph}})$. For each value of V, N_s and the overlaps were then calculated. The calculation of J_i and σ_i then depends only on the P_0 parameters. There are two elastic transfer rates P_{0z} and P_{0xy} and three phonon-assisted rates to X_{xy}: $P_{0xy}(\mathrm{TA})$, $P_{0xy}(\mathrm{LO_{Ga}})$, and $P_{0xy}(\mathrm{LO_{Al}})$. The $P_{0z}(\mathrm{ph})$ rates are given by the X_{xy} values corrected for the different final density of states [$P_{0z}(\mathrm{ph}) \approx 0.25\, P_{0xy}(\mathrm{ph})$].

We first present the results for Γ-X_z elastic transfer (dashed lines in Fig. 3), assumed in much previous work to be dominant.[8–10] It is seen that only some of the experimental features can be explained. However, when phonon-

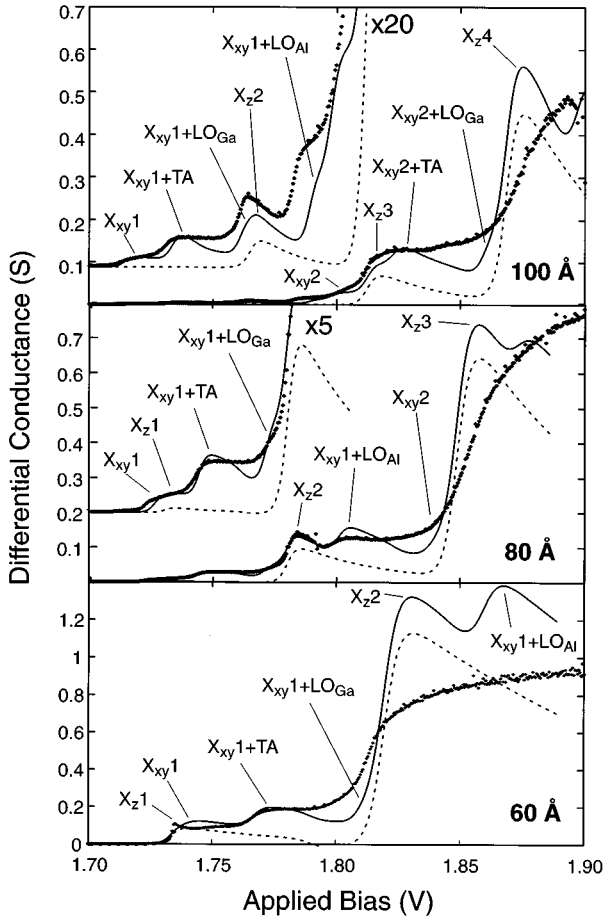

FIG. 3. Experimental σ-V data (dots) for the three samples and the theoretical conductance (solid lines) from the model described in the text. Their comparison allows the assignment of each experimental feature to a given intervalley transfer process. The dashed lines show the theoretical conductance including only elastic transfer to the X_z states.

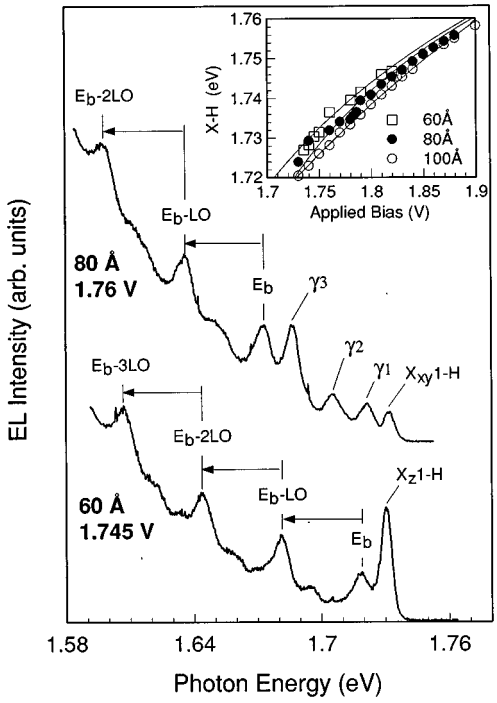

FIG. 4. EL spectra for the 60- and 80-Å samples showing the type-II luminescence and the typical signal from a highly monoenergetic hot electron population E_b. Inset: Evolution of the type-II X-H transition energy with bias. The solid lines are the fits discussed in the text.

assisted transfer is included the calculation describes all the σ-V features very well for all samples (the full lines on Fig. 3) and allows their clear identification.

To adjust the X_z resonances to fit the data we varied the conduction-band discontinuity between the Γ band edge in GaAs and the X band edge in AlAs ($\Delta_{\Gamma\text{-}X}$), which determines the biases at which resonances occur, and P_{0z} which determines their amplitude. It is important to note that the relative amplitude of the transfers to successive X_z levels is very well described by the model. This depends only on the overlaps and is not adjustable. The best fit is obtained for $P_{0z}=7\pm2$ ps^{-1} for all samples. The $\Delta_{\Gamma\text{-}X}$ values employed are 114 meV for 60 Å, 126 meV for 80 Å, and 123 meV for the 100-Å sample. They are in good agreement with that suggested by Mendez *et al.*[6] and are much less than the commonly used value of ~180 meV.[16]

The fitting to the X_{xy} resonance was obtained using the same $\Delta_{\Gamma\text{-}X}$ values. The best fits are obtained for $P_{0xy}(\mathrm{TA})=0.5\pm0.2$ ps^{-1}, $P_{0xy}(\mathrm{LO_{Ga}})=0.9\pm0.3$ ps^{-1}, and $P_{0xy}(\mathrm{LO_{Al}})=3\pm1$ ps^{-1} for all samples. For the 80- and 100-Å samples where X_{xy} is lowest the amplitude of the first conductance threshold is underestimated using the above value of P_{0z}. If we include an elastic transfer rate $P_{0xy}=0.15\pm0.05$ ps^{-1} to $X_{xy}1$ better agreement is obtained. For the 100-Å sample the same value of P_{0xy} accounts well for the feature at 1.80 V ascribed to elastic transitions to $X_{xy}2$. The relative values of the P_{0xy} and P_{0xy}(ph) parameters are in good agreement with those observed in X_{xy}-like type-II luminescence,[2,12] and with the relative intensities of the γ_i lines observed in EL, described below. The prominence of the X_{xy} resonances relative to X_z is notable. This is well described by the model and arises because of the much greater overlap of the X_{xy} states with the Γ emitter states in finite electric field. The strong contribution from X_{xy} was completely unsuspected in previous studies of transport through AlAs barriers, which were based primarily on comparison with type-II PL results at zero electric field.

The above analysis has permitted a precise determination of the transfer rates for elastic and phonon-assisted intervalley scattering. These are *intrinsic* values independent of the details of the structure. Using the relevant envelope function overlap, the intervalley transfer rates can then be calculated for other heterostructures. We applied these results to SL's of Ref. 5 and found very good agreement with the measured transfer times. For example, for sample 1 of Ref. 5, our calculation gives 0.17 ps compared to 0.14 ps measured, and for sample 8 of Ref. 5, 1.7 ps compared to 2.6 ps measured.

These $\Gamma\rightarrow X$ intervalley transfer mechanisms, which depend strongly on the nature (X_z or X_{xy}) of the X state, are confirmed by the EL measurements, which probe the complementary $X\rightarrow\Gamma$ transfer. Figure 4 presents typical EL spectra for the 60- and 80-Å samples. For the 60-Å sample X_z1 is the lowest state. We observe a strong no-phonon

type-II line X_z1-H, arising from recombination of X_z1 electrons with HAL (see Fig. 1). In addition, a hot electron population which relaxes by emitting a cascade of zone-center GaAs LO phonons ($\hbar\Omega_{\mathrm{LO},\Gamma}=36$ meV) is observed from its recombination with neutral acceptors (series of lines E_b-nLO, $n=0,\ldots,3$ in Fig. 4). As shown in Ref. 13 for $Al_xGa_{1-x}As$ barrier samples, the acceptor levels are shifted from the confined level in the HAL by about 13 meV. We observe the same shift between X_z1-H and E_b. This indicates that electrons are injected into the collector at the X_z1 energy. Thus we conclude that X_z to Γ transfer out of the barrier is elastic, in agreement with the conclusion for the Γ-X_z transfer.

For 80 Å (and in a similar way for 100 Å), $X_{xy}1$ is the lowest state and the type-II EL exhibits a weak no-phonon line $X_{xy}1$-H and three phonon replicas γ_1, γ_2, and γ_3 arising from pnonon-assisted recombination with the HAL, involving AlAs, TA, GaAs LO, and AlAs LO zone-boundary phonons, respectively. A zone-center GaAs LO-phonon cascade is again observed, the highest-energy line (E_b) being observed 13 meV below the γ_3 replica. We conclude in this case that the hot electrons are injected at an energy $\hbar\Omega_{\mathrm{LO,Al}}$ below $X_{xy}1$, thus showing that the dominant X_{xy}-Γ tunneling out mechanism is AlAs X point LO-phonon scattering, again in agreement with the conclusion for Γ-X_{xy} transfer.

No EL is observed at higher energy than X_z1-H or $X_{xy}1$-H, even for biases corresponding to the higher resonances in the conductance. This proves that intravalley relaxation in the AlAs is much more efficient than X to Γ tunneling out, which only occurs for electrons which have relaxed to the lowest X state. Thus tunneling through such indirect gap barriers is strongly sequential. Coherent tunneling induced by X_z-Γ mixing discussed in much previous work[8–10] appears to play very little role in the transport.

We also calculated the X-H transition energies using the self-consistent band potential. Good agreement with experiment is obtained using $\Delta_{\Gamma\text{-}X}$ of 116 meV for 60 Å, 115 meV for 80 Å, and 122 meV for 100 Å (inset to Fig. 4). This strongly confirms the value $\Delta_{\Gamma\text{-}X}=120\pm6$ meV. The type-II energy X-H is very sensitive to charge accumulation in the AlAs. The good agreement indicates that such charge buildup is small ($<10^{11}\,\mathrm{cm}^{-2}$), justifying the assumption made in the modeling of σ-V.

In conclusion, we have shown that Γ-X and X-Γ intervalley transfer in AlAs/GaAs 2D systems depends strongly on the nature (X_z or X_{xy}) of the X states involved, but with comparable strength in the two cases. Transfer to or from X_z is mainly elastic but not coherent, whereas transfer to or from X_{xy} is dominated by zone-boundary phonon scattering. In both cases Γ-X-Γ transport through indirect-gap AlAs barriers is sequential.

[1] P. Dawson, K. J. Moore, C. T. Foxon, G. W. 't Hooft, and R. P. M. van Hal, J. Appl. Phys. **65**, 3606 (1989).

[2] D. Scalbert, J. Cernogora, C. Benoit à la Guillaume, M. Maaref, F. F. Charfi, and R. Planel, Solid State Commun. **70**, 945 (1989).

[3] M. H. Meynadier, R. E. Nahory, J. M. Worlock, M. C. Tamargo, J. L. de Miguel, and M. D. Sturge, Phys. Rev. Lett. **60**, 1338 (1988).

[4] J. Feldmann, R. Sattmann, E. Göbel, J. Kuhl, J. Hebling, K. Ploog, R. Muralidharan, P. Dawson, and C. T. Foxon, Phys. Rev. Lett. **62**, 1892 (1989); J. Feldman *et al.*, Phys. Rev. B **42**, 5809 (1990).

[5] B. Deveaud, F. Clérot, A. Regreny, R. Planel, and J. M. Gérard, Phys. Rev. B **49**, 13 560 (1994).

[6] E. E. Mendez, W. I. Wang, E. Calleja, and C. E. T. Gonçalves da Silva, Appl. Phys. Lett. **50**, 1263 (1987).

[7] R. Beresford, L. F. Luo, W. I. Wang, and E. E. Mendez, Appl. Phys. Lett. **55**, 1555 (1989).

[8] D. Landheer, H. C. Liu, M. Buchanan, and R. Stoner, Appl. Phys. Lett. **54**, 1784 (1989).

[9] Y. Charbonneau, J. Beerens, L. A. Cury, H. C. Liu, and M. Buchanan, Appl. Phys. Lett. **62**, 1955 (1993).

[10] H. C. Liu, Appl. Phys. Lett. **51**, 1019 (1987).

[11] E. Finkman, M. D. Sturge, and M. C. Tamargo, Appl. Phys. Lett. **49**, 1299 (1986).

[12] H. W. van Kesteren, E. C. Cosman, P. Dawson, K. J. Moore, and C. T. Foxon, Phys. Rev. B **39**, 13 426 (1989).

[13] R. Teissier, J. J. Finley, M. S. Skolnick, J. W. Cockburn, R. Grey, G. Hill, and M. A. Pate, Phys. Rev. B **51**, 5562 (1995).

[14] We used a transverse effective mass of $m_{xy}=0.28m_0$ deduced from magnetotransport resonances with X_z Landau levels (to be published), which is in good agreement with the conclusions of N. Miura, H. Yokoi, J. Kono, and S. Sasaki, Solid State Commun. **79**, 1039 (1991), and a longitudinal mass of $m_z=1.1m_0$.

[15] The inhomogenous broadening of the confined levels was taken to be Gaussian of width 4 meV.

[16] G. Danan, B. Etienne, F. Mollot, R. Planel, A-M. Jean-Louis, F. Alexandre, B. Jusserand, G. Le Roux, J. Y. Marzin, H. Savary, and B. Sermage, Phys. Rev. B **35**, 6207 (1987).